Journal of Engineering Mathematics **35:** 251–272, 1999.

The draining of a two-dimensional bubble

P. D. HOWELL
Mathematical Institute, 24–29 St Giles', Oxford OX1 3LB, U.K.

Received 17 February 1997; accepted in revised form 31 May 1998

Abstract. A two-dimensional bubble at rest near the surface of a semi-infinite liquid layer is considered. A lubrication analysis of the thin film above the bubble is matched to a capillary-static solution for the outer geometry. Analysis of a transition region between the thinning viscous film and the capillary-static solution leads to an effective boundary condition to be applied at the edge of the film. The result is a description of the drainage of liquid out of the film under gravity and surface tension. This drainage is ultimately responsible for rupture of the film and hence bursting of the bubble.

Key words: bubbles, thin liquid films, surface tension, asymptotic expansions.

1. Introduction

During the manufacture of glass, 'batch', consisting mainly of sand, is introduced onto a heated bath of molten glass. It gradually floats along the bath, melting as it does so. The melting inevitably results in the formation of a large number of small bubbles. Further bubbles may be introduced by furnace equipment or contamination as the glass moves through the furnace. It is important that these all rise to the surface of the glass and burst before the glass leaves the furnace. It is far from clear to what extent a glass surface at furnace temperatures is affected by surface active agents, but at least in the first instance it is of interest to determine how long a bubble might take to burst at the surface of a viscous liquid assuming a constant surface tension.

In this paper we consider the final stage of the bursting process, when the bubble has already risen to the surface of the glass. It can remain there for some time while the thin liquid film that separates the bubble from the air above thins under the action of gravity and surface tension. Eventually the film becomes thin enough (around 1000Å) that inter-molecular (van der Waals) forces take over and the film rapidly ruptures, *i.e.* the bubble bursts.

Several previous authors have considered bubble rise towards a rigid or free surface and the film drainage problem that follows. The most satisfactory asymptotic study is that of Jones and Wilson [1] who considered the draining of the thin film above a solid sphere or liquid drop at a free surface. Their work is not valid, however, as the viscosity of the drop tends to zero, which is the limit of interest here. Chi and Leal [2] used a boundary-integral method to solve the full problem numerically. They found good agreement with [1] for small viscosity ratio, but not for large viscosity ratio (the regime of interest to us). Numerical solutions for nonzero Reynolds number were found by Shopov and Minev [3] using finite elements.

In many other papers (for example [4, 5, 6, 7, 8]) lubrication theory is used to model the film thinning problem (the last two also incorporating van der Waals forces). In each case a no-slip boundary condition is applied to at least one surface of the film, either because it is on a rigid or slightly mobile substrate, or because the free surface is assumed to be loaded with

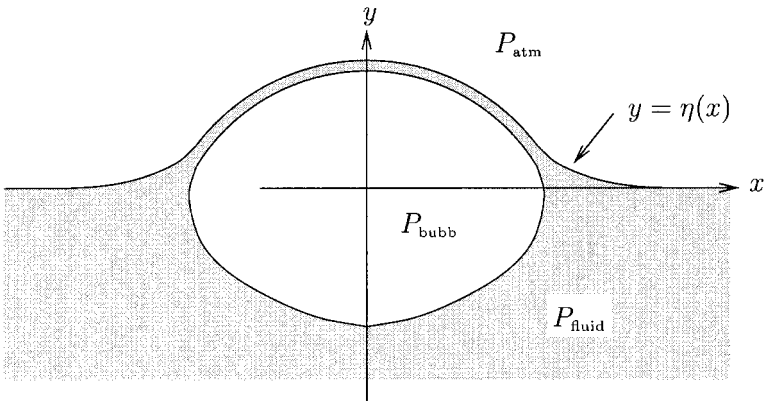

Figure 1. Schematic of a bubble at a liquid free surface.

surfactant. The resulting equations of motion, which are generalised versions of the standard lubrication equation [9] differ markedly from our governing Equations (21–23), since in our case both free surfaces are free and the flow is extensional [10].

Similar extensional flow models have been applied to macroscopic liquid films by Pearson and Petrie [11] and van de Fliert *et al.* [12] for example. To model much thinner films (for example lamellae), van der Waals forces were incorporated by Erneux and Davis [13], Hwang *et al*. [14] and Ida and Miksis [15, 16], while the effects of an insoluble surfactant were included by De Witt *et al.* [17] and Hwang *et al*. [18]. We sketch the derivation of a general model for the flow of a free liquid film under surface tension and gravity in Appendix A.

Our new contribution is to match such a model with an outer solution away from the bubble and hence quantify drainage out of the edge of the film. We use the concept of a transition region between the thin film and an outer capillary-static region: an idea similar to that applied to lubrication flows by Bretherton [19] and subsequent authors. Instead of including intermolecular forces, we make the simpler assumption that there is a critical thickness below which the film will rupture. To simplify matters further, in the body of the paper we restrict our attention to a two-dimensional geometry, which means that the capillary-static outer problem can be solved exactly. We show in Appendix B that qualitatively similar results occur for an axisymmetric configuration.

In Section 2 we derive the outer solution for a bubble of effectively zero thickness at a free surface. Then, in Section 3 we consider the flow of liquid in the thin cap of the bubble. For small Bond number we effect a decomposition of the flow into a nearly uniform thinning film and a transition region at its edge that matches with the outer solution from Section 2. The transition region supplies an effective boundary condition to be applied to a simple model for the thinning of the main part of the film. An exact solution of this model allows us to estimate the lifetime of a bubble at the surface of a viscous liquid. For non-small Bond number the matching procedure fails and a new approach is suggested in Section 4.

2. Capillary-static solution

Consider a two-dimensional gas bubble almost at rest at a liquid free surface, as shown in Figure 1. We employ Cartesian coordinates with the y-axis pointing vertically upwards along the axis of the bubble. The free surface is given by $y = \eta(x)$, and the origin is chosen such

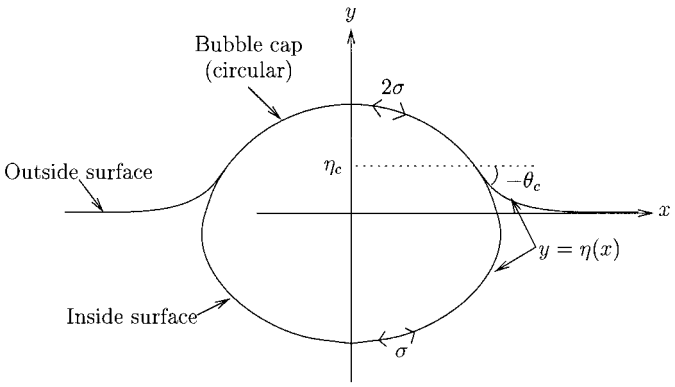

Figure 2. The capillary-static outer problem.

that $\eta \to 0$ as $x \to \infty$. Our fundamental assumption is that the liquid film at the top of the bubble is thin compared to the bubble radius. As a result, we can decompose the liquid domain into three regions which are analysed separately. In this section we find the outer solution on a scale on which the film has zero thickness and capillary statics dominates. This means that the problem reduces to the solution of the Laplace–Young equation for $\eta(x)$.

In the idealised static situation shown in Figure 2, the film on top of the bubble has zero thickness, but nevertheless a surface tension $2\,\sigma$ while the other free surfaces have a surface tension σ. The three curves are all tangent at their common point of intersection. The radius of curvature of the thin film is given by a balance between the pressure drop across it (assumed constant) and surface tension:

$$R = \frac{2\sigma}{\Delta P}, \quad \text{where } \Delta P = P_{\text{bubb}} - P_{\text{atm}}, \tag{1}$$

and in terms of this radius we define a Bond number

$$\mathrm{B} = \frac{\rho g R^2}{\sigma} = \frac{4\rho g \sigma}{\Delta P^2}. \tag{2}$$

Here ρ is the density difference between the liquid and gas phases and g is the acceleration due to gravity. Note that R is *not* the radius of the bubble – for nonzero Bond number the bubble is not circular and so does not have a well-defined radius. However, R *is* related to bubble size, in a way that we will find later.

The free surfaces outside (denoted by the subscript 'out') and inside (denoted by the subscipt 'in') satisfy the Laplace–Young equation, which relates their curvature κ to hydrostatic pressure, and reads in either case

$$\sigma\kappa_{\text{out}} = \rho g \eta, \qquad \sigma\kappa_{\text{in}} = \Delta P + \rho g \eta. \tag{3}$$

These are best solved using an angle/arc-length formulation. We define θ to be the angle made by the free surface with the x-axis in either case, and s to be arc-length along the surface. Our approach is to solve first for the 'outside' free surface and then to patch the solution to that for the 'inside' surface. Finally, the patching of both solutions to the circular cap results in a unique bubble shape for each value of B.

2.1. THE 'OUTSIDE' SURFACE

When we nondimensionalise all lengths with R and use an angle/arc-length formulation, the governing equations for the free surface read

$$\frac{\partial\theta}{\partial s} = \mathrm{B}\eta, \qquad \frac{\partial\eta}{\partial s} = \sin\theta. \tag{4}$$

Without loss of generality we take $s = 0$ to be the point of intersection, and denote the angle made by the free surface there by θ_c. Then the solution of (4) with $\theta \to 0$, $\eta \to 0$ as $s \to \infty$ is [20, Section 127]

$$\theta = 4\tan^{-1}\left[\tan\left(\frac{\theta_c}{4}\right)\exp(-s\sqrt{\mathrm{B}})\right]. \tag{5}$$

Hence we obtain a relation between the free surface angle θ_c and height, say η_c, at the intersection point

$$\eta_c = -\frac{2}{\sqrt{\mathrm{B}}}\sin\left(\frac{\theta_c}{2}\right). \tag{6}$$

This is the classical solution for capillary rise up a vertical wall with contact angle θ_c, *e.g.* [21, Section 1.9].

2.2. THE 'INSIDE' SURFACE

The inside free surface feels an extra component of pressure arising from the jump ΔP, and therefore satisfies

$$\frac{\partial\theta}{\partial s} = 2 + \mathrm{B}\eta, \qquad \frac{\partial\eta}{\partial s} = \sin\theta. \tag{7}$$

Here we take the origin for s to be the bottom of the bubble and denote the intersection point by $s = s_c$, so the boundary conditions are

$$\theta = 0, \quad \text{at} \quad s = 0, \tag{8}$$

$$\theta = \pi + \theta_c, \qquad \eta = \eta_c \quad \text{at} \quad s = s_c. \tag{9}$$

The solution is an elliptic integral [20, Section 127]

$$\int_0^{\theta/2} \frac{\mathrm{d}\tau}{\sqrt{1 + a^2\sin^2\tau}} = \frac{\sqrt{\mathrm{B}}}{a}s, \tag{10}$$

where

$$a^2 = \frac{\mathrm{B}}{2\mathrm{B}\sin^2\frac{1}{2}\theta_c - 2\sqrt{\mathrm{B}}\sin\frac{1}{2}\theta_c + 1 - \mathrm{B}}. \tag{11}$$

The conditions for this solution to exist are

$$-\pi \leqslant \theta_c \leqslant 0 \quad \text{for} \quad \mathrm{B} < 1,$$

$$-\pi \leqslant \theta_c < -\beta \quad \text{for} \quad \mathrm{B} \geqslant 1,$$

where

$$\tan\beta = \frac{\mathrm{B}-1}{\sqrt{2\mathrm{B}-1}}.$$

From the above solution we can also obtain the horizontal distance x_c of the point of intersection from the centre of the bubble

$$x_c = \int_0^{s_c} \cos\theta \, \mathrm{d}s. \tag{12}$$

Since the bubble cap is a circular arc of dimensionless radius one, x_c must be equal to $-\sin\theta_c$, and hence we obtain a functional relation between θ_c and B

$$(2-k^2)\mathrm{F}(\phi;k) - 2\mathrm{E}(\phi;k) = \frac{k\mathrm{B}\sin\theta_c \sin\frac{1}{2}\theta_c}{1-\sqrt{\mathrm{B}}\sin\frac{1}{2}\theta_c}, \tag{13}$$

where F and E are elliptic integrals of the first and second kind respectively, with modulus and amplitude given by

$$k^2 = \frac{a^2}{1+a^2} = \frac{\mathrm{B}}{1-2\sqrt{\mathrm{B}}\sin\frac{1}{2}\theta_c + 2\mathrm{B}\sin^2\frac{1}{2}\theta_c},$$

$$\sin\phi = \frac{\sqrt{\mathrm{B}}\cos\frac{1}{2}\theta_c}{k(1-\sqrt{\mathrm{B}}\sin\frac{1}{2}\theta_c)}.$$

In Figure 3 we plot θ_c against B. From this we deduce that θ_c always lies between $-\pi/2$ and 0: there are no solutions in which the bubble sits proud of the surface as shown in Figure 4(*iv*). As the Bond number (*i.e.* the dimensionless bubble size) approaches zero, $\theta_c \to 0$ so that the bubble approaches a circle beneath a flat surface. The value of θ_c decreases monotonically with B, approaching $-\pi/2$ for very large bubbles. The variation of the bubble shape with B is shown schematically in Figure 4.

From the bubble shape, we can determine its area (which corresponds to volume in this two-dimensional configuration), nondimensionalised with R^2

$$A = \sin\theta_c - \theta_c - 2\sin\theta_c\left[\sin\left(\frac{\theta_c}{2}\right) - \frac{1}{\sqrt{\mathrm{B}}}\right]^2. \tag{14}$$

By combining (14) with (13) we obtain a functional relation between the bubble area A and B, plotted in Figure 5. As noted above, the bubble approaches a circle when $\mathrm{B} \to 0$, but notice that the radius of that circle is $R/2$ not R. To close the equations and enable us to determine B (and hence R, A and θ_c), we assume a gas law is given that relates the bubble area to the pressure inside it. The simplest such law is to assume that the gas in the bubble is incompressible, so that the bubble area is fixed at some given initial value A_0. In this case,

$$R = \sqrt{\frac{\sigma}{\rho g}} f\left(\frac{\rho g A_0}{\sigma}\right), \tag{15}$$

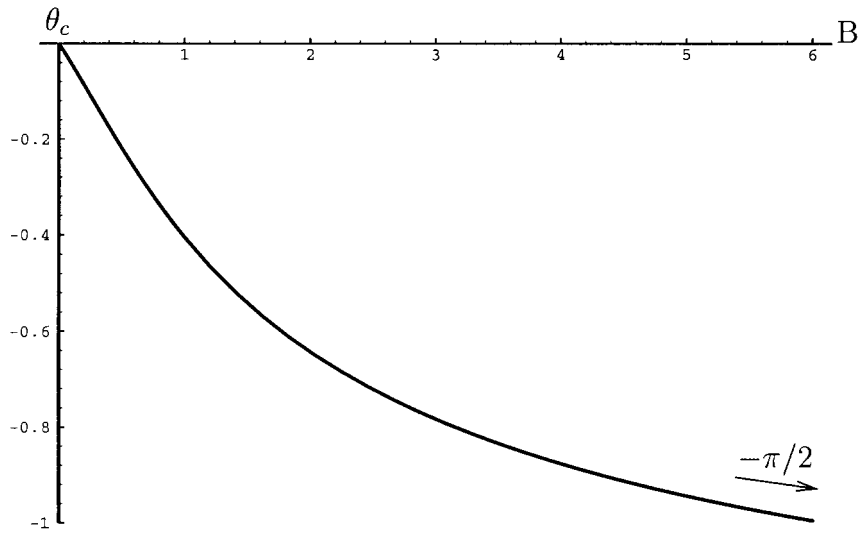

Figure 3. Angle at which fluid interfaces meet, θ_c, against Bond number.

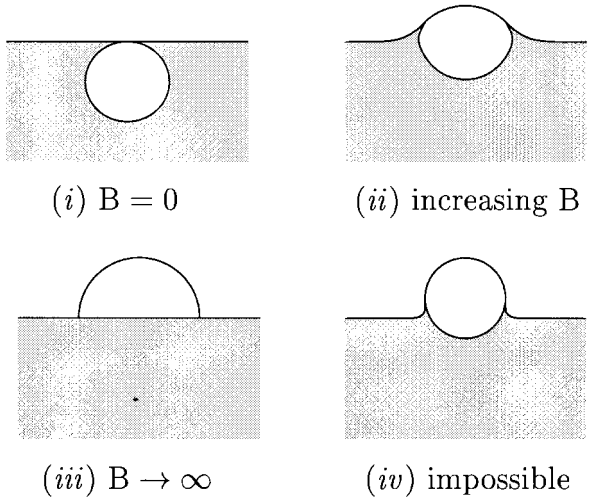

Figure 4. Schematic of the variation of bubble shape with Bond number.

where the function $f(\,\cdot\,)$, obtained by inverting (14), is plotted in Figure 6.

For many bubbles of practical interest, the expressions found heretofore can be simplified somewhat by assuming that the Bond number is small (for a bubble in molten glass, for example, this will be true if the radius is around a millimetre or less). This allows us to express θ_c and A as asymptotic expansions in B

$$\theta_c \sim -\frac{\pi}{8}\mathrm{B} - \frac{3\pi}{32}\mathrm{B}^2 + \frac{\pi^2}{32}\mathrm{B}^{5/2} + O(\mathrm{B}^3), \tag{16}$$

$$A \sim \frac{\pi}{4} + \frac{\pi}{8}\mathrm{B} - \frac{\pi^2}{32}\mathrm{B}^{3/2} + O(\mathrm{B}^2). \tag{17}$$

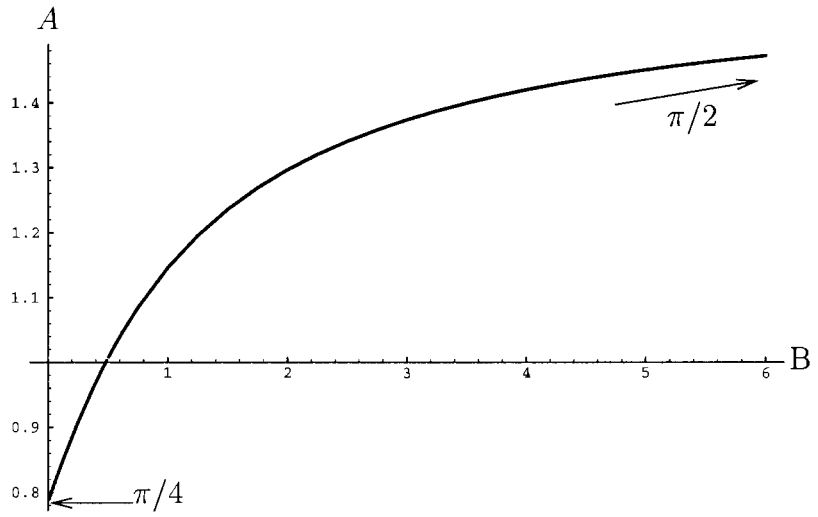

Figure 5. Dimensionless bubble area versus Bond number.

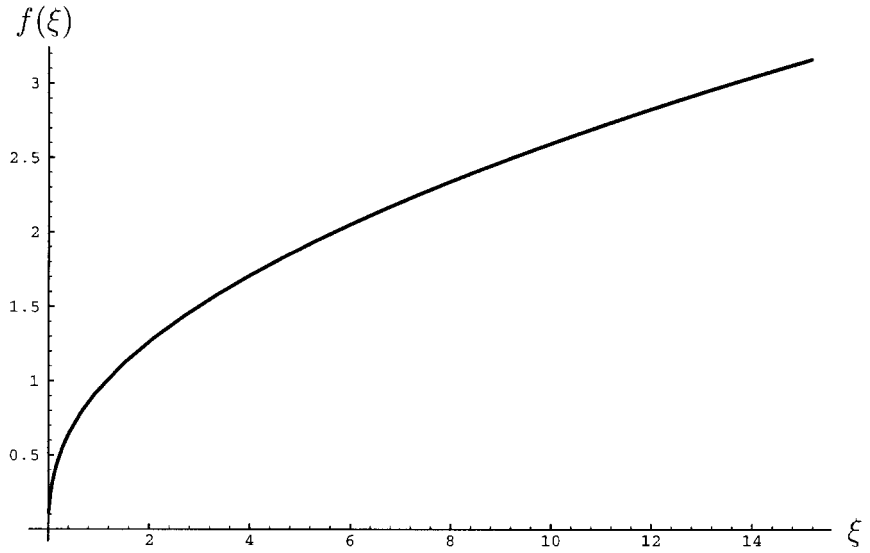

Figure 6. Function relating dimensionless bubble radius to dimensionless bubble area: $R = (\sigma/\rho g)^{1/2} f(\rho g A_0/\sigma)$.

Hence, given the dimensional bubble area A_0, and assuming $a = \rho g A_0/\sigma \ll 1$, we obtain R in the form

$$R \sim 2\sqrt{\frac{A_0}{\pi}} \left\{ 1 - \frac{a}{2\pi} + \frac{a^{3/2}}{2\sqrt{\pi}} + O(a^2) \right\}. \tag{18}$$

The result of the analysis of this section is that, given the size of a bubble, we can predict the radius of curvature R of, and angle $-\theta_c$ subtended by, the thin film on top of the bubble.

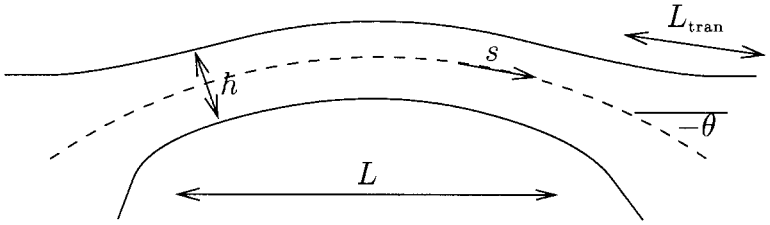

Figure 7. Schematic of a thin liquid film.

Moreover, for subsequent matching with the flow in the thin film, we will require the sum of the curvatures of the two surfaces where they intersect with the thin film:

$$\kappa_{\text{total}} = 2(1 + \text{B}\eta_c) = 2 - 4\sqrt{\text{B}} \sin\left(\frac{\theta_c}{2}\right). \tag{19}$$

3. Thin-film analysis

Here we model the flow in the thin liquid film capping the bubble, as shown in Figure 7. As previously, we use arc-length s and angle θ to describe the centre-line of the film (whose curvature is given by $\kappa = \theta_s$), and denote the film thickness by $h(s, t)$ and the axial fluid velocity by $u(s, t)$. The radius of curvature R and length scale L of the film are given by the solution of the outer problem discussed in Section 2. We write the governing equations in dimensionless form, using the following scalings:

$$h = h_0 h', \qquad s = Rs', \qquad u = Vu', \qquad t = (R/V)t'. \tag{20}$$

We take the origin of s to be the centre of the film, so that the edge is at $s = s_c = -\theta_c$.

The general equations for the flow of viscous liquid in a thin film under surface tension and gravity are given in Appendix A. For a two-dimensional film, these reduce to (dropping primes)

$$h_t + (uh)_s = 0, \tag{21}$$

$$\text{Ca}(4hu_s)_s + \frac{\epsilon}{2} h(h_{sss} + \theta_s^2 h_s) = \text{B}\, h \sin\theta, \tag{22}$$

$$(1 + 2\epsilon\text{Ca}\, hu_s)\theta_s = -1 + \frac{\epsilon\text{B}}{2} h \cos\theta, \tag{23}$$

where the capillary number is defined by $\text{Ca} = \mu V/\sigma$, and the inverse aspect ratio is $\epsilon = h_0/R \ll 1$. Physically, these equations correspond to conservation of mass and tangential and normal force balances respectively. Not all the terms in (21–23) can balance at once – depending on the relative sizes of the dimensionless parameters, certain physical effects will be negligible in all or part of the film, so that the corresponding terms can be omitted. In particular, we anticipate that the surface tension effects in (22) are small in the main body of the film, where variations in h are small, but become important towards the edge of the film $s = s_c$, where h begins to increase rapidly. This motivates a decomposition of the fluid into an unsteady thinning film away from the edges where surface tension is negligible, and

a quasi-steady transition region near the edges where surface tension becomes important and the free surfaces match with the outer solution found in Section 2.

The normal force balance (23) gives

$$\frac{\partial \theta}{\partial s} + 1 \sim O(\epsilon \mathrm{Ca}, \epsilon \mathrm{B}),$$

and since it will transpire that both terms on the right-hand side are small, this simply implies that the film forms a circular arc, as assumed in Section 2.

For the remainder of this section we assume $\mathrm{B} \ll 1$. This simplifies the analysis greatly, for reasons that are discussed in Section 4. Then, using (16) we see that the length of the film scales with $\mathrm{B}R$, which motivates the rescaling

$$s = \mathrm{B}\varsigma, \qquad \theta = \mathrm{B}\phi, \qquad t = \mathrm{B}\tau, \tag{24}$$

after which the edge of the film is given by $\varsigma = \varsigma_c$, where

$$\varsigma_c \sim \frac{\pi}{8} + \frac{3\pi}{32}\mathrm{B} + O(\mathrm{B}^{3/2}).$$

3.1. The transition region

The length scale of the transition region is determined by the fact that it must match with the thin film on one side and with the outer solution of Section 2 on the other. The solution for h in this region is expected to be quadratic 'at infinity', to be matched with the curvature κ_{total} found in the previous section. The matching can only be achieved if the transition length scale is chosen to be

$$L_{\mathrm{tran}} = \sqrt{h_0 R}, \tag{25}$$

and a balance between surface tension and viscous stress in this region gives the velocity scale.

$$V = \frac{\sigma}{\mu}\sqrt{\epsilon}. \tag{26}$$

For the concept of a transition region to be useful, we require L_{tran} to be much less than the length of the film, and this leads to the condition

$$\epsilon \ll \mathrm{B}^2 \ll 1. \tag{27}$$

In the transition region, we set

$$s = s_c + \sqrt{\epsilon} S \quad \text{or equivalently} \quad \varsigma = \varsigma_c + \frac{\sqrt{\epsilon}}{\mathrm{B}} S,$$

and denote the dependent variables with capital letters also. Employing the scales (25, 26), we obtain

$$\frac{\sqrt{\epsilon}}{\mathrm{B}} H_\tau + (UH)_S = 0, \tag{28}$$

$$(4HU_S)_S + \frac{H}{2}H_{SSS} \sim O(\epsilon, \mathrm{B}\sqrt{\epsilon}). \tag{29}$$

The boundary conditions are found by matching with the main film on one side and the outer solution from Section 2 on the other

$$H \to h(\varsigma_c), \qquad U \to u(\varsigma_c) \quad \text{as} \quad S \to -\infty, \tag{30}$$

$$H_{SS} \to \kappa_{\text{total}} \quad \text{as} \quad S \to +\infty. \tag{31}$$

Note that if $\epsilon \sim O(\mathrm{B}^2)$ then (28, 29) is the time-dependent problem including surface tension, which implies that surface tension is important throughout the film. However, the quasi-steady verion that results from the Assumption (27) can be integrated analytically. From (28),

$$HU = h(\varsigma_c)u(\varsigma_c), \tag{32}$$

and then, integrating (29) twice and applying conditions at $S \to -\infty$, we obtain

$$HH_S = \frac{16u(\varsigma_c)}{3\sqrt{h(\varsigma_c)}}(H^{3/2} - h(\varsigma_c)^{3/2}). \tag{33}$$

Another integration can be performed, but for our purposes it is only necessary to make use of the behaviour of H as $S \to +\infty$. The result is a relation between $u(\varsigma_c)$, $h(\varsigma_c)$ and κ_{total}

$$u(\varsigma_c) = \frac{8}{3}\sqrt{\frac{\kappa_{\text{total}}h(\varsigma_c)}{2}}. \tag{34}$$

This is the boundary condition to be applied to the film at its edge. Physically, the negative pressure at the edge of the film acts as a sink sucking fluid out of the film. The rate at which it does so is given by (34).

3.2. The thinning film

After the rescaling (24), the leading-order governing equations in the main film become

$$h_\tau + (uh)_\varsigma = 0, \tag{35}$$

$$(4hu_\varsigma)_\varsigma - \frac{\mathrm{B}^4}{\sqrt{\epsilon}}h\phi \sim O\left(\mathrm{B}^2, \frac{\sqrt{\epsilon}}{\mathrm{B}}\right). \tag{36}$$

Again we note that the assumption $\epsilon \ll \mathrm{B}^2$ is required for surface tension to be negligible in (36). The second term in (36), which represents gravity, will also be neglected henceforth. For a bubble in molten glass with a radius of around a millimetre, for example, this term would only become considerable if the thickness dropped to 0·1Å, long before which the film would have ruptured.

We assume symmetry of the film about $\varsigma = 0$,

$$u = 0 \quad \text{at } \varsigma = 0, \tag{37}$$

Table 1. Estimated parameter values for a bubble in molten glass.

Property	Symbol	Approximate value	Units
Viscosity	μ	2500	N s m^{-2}
Density	ρ	10^3	Kg m^{-3}
Gravitational accel.	g	10	m s^{-2}
Surface tension	σ	10^{-1}	N m^{-1}
Initial thickness	h_0	10^{-5}	m
Rapture thickness	h_{rup}	10^{-7}	m
Bubble cap radius	R	10^{-3}	m
Rupture timescale	t_{rup}	60	s

and the boundary condition (34) derived via matching with the transition region, along with an initial condition for h, closes the system.

The problem (35–37, 34) is particularly easy to solve if the film is taken to be uniform initially (say $h \equiv h_0$ at $t = 0$). Then h remains uniform and the solution in dimensional form is

$$\frac{h}{h_0} = \left(1 + \frac{32}{3\pi}\frac{\sigma^2}{\mu\rho g}\frac{h_0^{1/2}}{R^{7/2}}t\right)^{-2}. \tag{38}$$

Hence, if the thickness at which the film raptures is h_{rup}, then the time taken for the bubble to burst is

$$t_{\text{rup}} = \frac{3\pi}{32}\frac{\mu\rho g}{\sigma^2}R^3\left(\sqrt{\frac{R}{h_{\text{rup}}}} - \sqrt{\frac{R}{h_0}}\right), \tag{39}$$

which has the implication that smaller bubbles should burst much faster than larger ones. Recall that this result was obtained in the limit $\sqrt{h_0/R} \ll \rho g R^2/\sigma \ll 1$. The time taken for the film thickness to become small enough for (38) to apply may be considerable, and may well be longer for smaller bubbles.

For bubbles in molten class, the dimensional parameters, in particular surface tension and viscosity, are strongly temperature-dependent, and so may vary considerably depending on the stage in the forming process during which the bubble arrives at the free surface. However, using the rough estimates shown in Table 1, the rapture time is found to be approximately one minute.

4. Form of the problem for $B \sim O(1)$

The matching between the main film and the transition region carried out in the previous section is much more problematic if B is not assumed to be small. In such a case, the length

scale of the main film is R and the velocity scale is determined by a balance between viscous stress and gravity

$$V = \frac{\rho g R^2}{\mu}. \tag{40}$$

The governing equations for the main film therefore reduce to

$$h_t + (uh)_s = 0, \tag{41}$$

$$(4hu_s)_s + h \sin s = 0. \tag{42}$$

The velocity scale in the transition region is still given by a balance between viscosity and surface tension, and if the film thickness is to match quadratically with the outer solution, this necessarily leads to the scale (26), which is now much smaller than (40). The implication is that gravity causes fluid to drain into the transition region at a much faster rate than surface tension can suck it out.

This situation can be remedied, and (41, 42) rescued, by relaxing the assumption that the transition region be slender. If the film thickness is assumed to be *linear*, rather than quadratic, as it matches with the outer solution, then the velocity scales in the two regions can be reconciled. The appropriate length scale for the transition region is found to be

$$L_{\text{tran}} = \frac{h_0}{\mathrm{B}}. \tag{43}$$

This implies that in the outer problem of Section 2, the interfaces should actually meet with a finite angle, of order $\tan^{-1} \mathrm{B}$, rather than zero angle as assumed in Section 2. The transition region solution must match with that angle at positive infinity and with the solution of (41, 42) at minus infinity. Hopefully the extra boundary condition analogous to (34) could be deduced from the solution in the transition region and the matching conditions.

In this regime, no thin-film approximation can be employed in the transition region. Instead the full two-dimensional Stokes flow problem must be solved with surface tension on the free boundary. The problem is quasi-steady, and it is hoped that explicit solutions may be available via complex analysis techniques (see for example [22]). Otherwise a canonical problem must be solved numerically.

5. Conclusions

We have modelled the draining of a two-dimensional viscous bubble under gravity and surface tension. The leading-order solution is hydrostatic, with viscous effects negligible compared to gravity and surface tension. In the thin liquid film capping the bubble however, surface tension is assumed to be negligible, and viscous drag dominates. In between there is a transition region in which viscous drag and surface tension balance. In the parameter regime considered in this paper (chosen to be applicable to the bursting of small bubbles in liquid glass), the governing equations can be integrated analytically in the transition region, and provide an effective boundary condition to be applied at the edge of the thin film. We use this boundary condition to estimate the time taken for a bubble at the surface of a viscous liquid to rupture.

We expect the decomposition employed in this paper – into a thin draining film, a transition region and a capillary- or hydrostatic outer solution – and the effective boundary condition (34) to be widely applicable. An example is the thinning and eventual rapture of a lamella in a foam. Here the capillary-static Plateau border acts as a sink sucking fluid out of the edge of the lamella, and our theory can be applied directly.

However, the liquid component of most foams of practical interest is many orders of magnitude less viscous than liquid glass, and so our theory typically predicts extremely rapid collapse. This is indeed the behaviour one would expect from a foam constructed out of a pure liquid, and foams that exhibit much longer lifetimes must have some stabilising mechanism: usually one that involves surface tension gradients. These can arise in many ways, including (*i*) surfactant molecules that accumulate on the free surfaces, (*ii*) chemical gradients due to mass exchange between the liquid and gaseous phases, and (*iii*) thermal gradients due to differential heat exchange along the lamellae; see [23]. Each of these mechanisms may play a role in bubbles in glass also, and may help to explain why bubbles occasionally last much longer than the timescale predicted by (39).

Our analysis is simplified by considering a two-dimensional geometry. Since the azimuthal component of curvature is not large in the bubbles under consideration, one should expect the results to be qualitatively close to those of the true three-dimensional geometry. We confirm this in appendix B by performing the corresponding analysis for an axisymetric bubble. It is worth noting that the transition region is effectively two-dimensional, even for a three-dimensional bubble, since its lengthscale is much smaller than the bubble radius. Hence the boundary condition (34) applies to a three-dimensional bubble also. The same is true for the scenario discussed in Section 4: even for a three-dimensional bubble, only a two-dimensional Stokes flow problem need be solved.

Acknowledgements

I would like to thank Dr J. R. Ockendon and Mr D. Gelder for their helpful advice in the preparation of this paper. This work was funded by a Junior Research Fellowship from Christ Church, Oxford OX1 1DP, UK.

Appendix

A. Derivation of the thin-film equations

The reader is referred to [10] for a general discussion of the use of systematic asymptotic methods to derive reduced-dimension models for viscous flow in thin films. Here we give a rough outline of the method and of the general equations that it produces.

Consider a thin film of viscous fluid whose centre-surface is given parametrically by

$$\boldsymbol{r} = \boldsymbol{r}_c(x^1, x^2, t),$$

where x^1 and x^2 are spatial parameters and t is time. We use coordinates (x^1, x^2, n) to describe a point in the film whose position vector at time t is

$$\boldsymbol{r} = \boldsymbol{r}_c(x^1, x^2, t) + n\boldsymbol{n}(x^1, x^2, t),$$

where $\boldsymbol{n}$ is the unit normal to the centre-surface. Hence the two free surfaces are given by $n = \pm\frac{1}{2}h$, where $h(x^1, x^2, t)$, is the film thickness.

Now the method runs as follows.

1. Write down the Navier-Stokes equations and dynamic and kinematic boundary conditions on the two free surfaces, using the coordinate system (x^1, x^2, n). A thoughtful choice of spatial parametrisation makes this job easier.
2. Nondimensionalise x^1 and x^2 with a typical length scale R, and n with a typical thickness h_0. In our problem, the characteristic length is defined to be the cap radius

$$R = \frac{2\lambda\sigma}{\Delta P},$$

where λ is 1 in a two-dimensional geometry or 2 in an axisymmetric configuration. The inverse aspect ratio of the sheet is defined to be

$$\epsilon = \frac{h_0}{R} \ll 1.$$

Suppose also that velocity is scaled with a typical flow speed V and time with R/V.

3. Decide how the other dimensionless parameters scale with ϵ. In our case inertia is certainly neglible so the only parameters of interest are the capillary number and Bond number

$$\mathrm{Ca} = \frac{\mu V}{\sigma}, \qquad \mathrm{B} = \frac{\rho g L^2}{\sigma}.$$

4. Pose asymptotic expansions of the dependent variables in powers of the small parameter ϵ.
5. Expand the governing equations and boundary conditions in powers of ϵ. By equating the coefficients, deduce equations for the leading-order unknowns.

Step 3 is particularly of interest here since we do not know *a priori* what the velocity scale is, and hence how Ca scales with ϵ. Therefore, it is better to look for all the possible distinguished limits in which the different physical effects balance. One of these occurs when $\mathrm{Ca} \sim O(\epsilon^{-1})$, in which case surface tension and viscous effects are of the same order in the normal force balance, but surface tension is negligible in the tangential force balance; this limit is used in [12] to model the flow of glass sheets. The other extreme occurs when $\mathrm{Ca} \sim O(\epsilon)$, in which case surface tension balances viscosity in the tangential force balance, but surface tension dominates the normal force balance; this limit is used in [15] to model flow in a lamella. Outside these two extreme cases, either viscosity or surface tension is formally negligible throughout. Similar considerations apply to B: once again the two extreme cases are $\mathrm{B} \sim O(\epsilon^{\pm 1})$.

Having examined all the limiting cases, one can construct *uniformly valid* equations that contain the leading-order terms obtained in each limit. In this way we obtain equations that give the correct leading-order behaviour *however* Ca *and* B *scale with* ϵ. Since (to the author's knowledge) they do not appear elsewhere in print, we present the full equations here in a concise tensorial form that is valid in any coordinate system.

We denote the first and second fundamental forms of the centre-surface by $a_{ij}\,\mathrm{d}x^i\,\mathrm{d}x^j$ and $b_{ij}\,\mathrm{d}x^i\,\mathrm{d}x^j$ respectively (in each case $i, j = 1, 2$). and set $a = \det(a_{ij})$. If gravity acts in the direction $-\boldsymbol{k}$, we decompose this vector into normal and tangential components

$$k_n = \boldsymbol{k}.\boldsymbol{n}, \qquad \hat{\boldsymbol{k}} = \boldsymbol{k} - k_n\boldsymbol{n}. \tag{A1}$$

If the surface velocity of the liquid *relative to the moving coordinate system* is $\boldsymbol{u}$, then the rate-of-strain tensor ε is given by

$$2\varepsilon_{ij} = \frac{\partial a_{ij}}{\partial t} + u_{i,j} + u_{j,i}, \tag{A2}$$

and in terms of this, the surface viscous stress tensor $\boldsymbol{\sigma}(x^1, x^2, t)$ is found to be

$$\sigma_i^j = 2h(\varepsilon_k^k\delta_i^j + \varepsilon_i^j). \tag{A3}$$

The governing equations represent conservation of mass,

$$\frac{1}{\sqrt{a}}\frac{\partial}{\partial t}(\sqrt{a}h) + \boldsymbol{\nabla}_s(\hat{\boldsymbol{u}}h) = 0, \tag{A4}$$

tangential force balances in the x^1- and x^2-directions,

$$\mathrm{Ca}\boldsymbol{\nabla}_s.\boldsymbol{\sigma} + \frac{\varepsilon}{2}h\boldsymbol{\nabla}_s[\nabla_s^2 h + b_{ij}b^{ij}h] = \mathrm{B}h\hat{\boldsymbol{k}}, \tag{A5}$$

and a normal force balance.

$$2b_j^j + \epsilon\mathrm{Ca}\sigma^{ij}b_{ij} = -2\lambda + \epsilon\mathrm{B}k_n h, \tag{A6}$$

where $\boldsymbol{\nabla}_s$ is the surface gradient operator. Note that the components of the tensor σ^{ij} and vector u^i do *not* correspond to the physical components of stress and velocity, which are given respectively by

$$\sigma(ij) = \sqrt{\frac{a_{ii}}{a_{jj}}}a_{jm}\sigma^{im}, \quad u(i) = \sqrt{a_{ii}}u^i,$$

see [24] for example.

In (A4–A6) we have four equations for the nine unknowns h, u_i, a_{ij} and b_{ij}. Three more equations, known as the formulae of Mainardi–Codazzi and the equation of Gauss, arise from conditions for compatibility between the first and second fundamental forms. Therefore two degrees of freedom remain, corresponding to the arbitrariness of our parametrisation (x^1, x^2): a particular choice of coordinates closes the system. Choices that might be useful include (*i*) Lagrangian coordinates (as in [11]), (*ii*) coordinates fixed with respect to the moving surface (as in [24]), or (*iii*) coordinates that remain orthogonal as the surface evolves (as in [10]).

Inspection of (A4–A6) elucidates the comments made earlier: it is impossible for surface tension to balance either gravity or viscous effects in both (A5) and (A6). We also note that there has been an implicit assumption that the typical radius of curvature of the film, R, is the same order as its length L. In practice we may well have $L \ll R$ and (A4–A6) will remain

valid so long as $h_0/L \ll 1$. (Similarly, we can allow $R \ll L$ so long as $h_0/R \ll 1$, although that limit is not of interest in this paper.)

B. Axisymmetric bubble bursting

Although the axisymmetric version of the problem tackled in this paper is qualitatively similar to the two-dimensional configuration, the analysis is hampered by the fact that the outer capillary-static problem cannot be solved explicitly. However, in this appendix we construct an asymptotic solution using the fact that the Bond number is small. As in Section 2 we decompose the bubble into an 'inside' free surface and an 'outside' free surface, both of which satisfy the Laplace–Young equation, and a (in this case) spherical cap. Because of the extra component of curvature, a normal force balance on the cap gives a radius

$$R = \frac{4\sigma}{\Delta P}, \tag{B1}$$

and we use this radius to nondimensionalise all lengths and to define the Bond number in this case. The 'inside' surface closely resembles a sessile drop, which has been analysed in the small Bond number limit by O'Brien [25], while the 'outside' surface is similar to the meniscus on a small cylinder [26, 27]. Similar small Bond number asymptotics were applied to holes in fluid layers by Wilson and Duffy [28].

We employ cylindrical polar coordinates (r, z) with the z-axis along the axis of symmetry of the bubble and pointing vertically upwards. The free surface is denoted by $z = \eta(r)$, and the origin for z is chosen such that $\eta \to 0$ as $r \to \infty$. As in Section 2, it is convenient to introduce the angle θ made by the free surface with the horizontal direction and arc length s measured along the free surface in the (r, z) plane. We begin with an analysis of the inside surface.

B.1. *The 'inside' surface*

The displacement of the free surface inside the bubble is governed by the system

$$\frac{\partial\theta}{\partial s} + \frac{\sin\theta}{r} = \mathrm{B}\eta + 4, \qquad \frac{\partial\eta}{\partial s} = \sin\theta, \qquad \frac{\partial r}{\partial s} = \cos\theta. \tag{B2}$$

The origin for s is chosen to be the bottom of the bubble, so we require

$$\theta(0) = r(0) = 0. \tag{B3}$$

We pose asymptotic expansions of the dependent variables in the form $\theta \sim \theta_0 + \mathrm{B}\theta_1 + \mathrm{B}^2\theta_2 + \cdots$, *etc*. The leading-order (zero Bond number) solution is simply a sphere resting under a flat free surface, whence

$$\theta_0 = 2s, \qquad \eta_0 = -\tfrac{1}{2}(1 + \cos 2s), \qquad r_0 = \tfrac{1}{2}\sin 2s. \tag{B4}$$

Proceeding to $O(\mathrm{B})$ and using (B3) we obtain the first-order solution:

$$\theta_1 = -\frac{3s + \sin 3s}{12\cos s}, \tag{B5}$$

$$\eta_1 = c_1 + \frac{\cos 4s - 5\cos 2s}{48} - \frac{s\sin 2s}{9} + \frac{\log(\cos s)}{12}, \tag{B6}$$

$$r_1 = \frac{5\sin 2s - \sin 4s}{48} - \frac{s\cos 2s}{8}, \tag{B7}$$

where c_1 is an (as yet) undetermined constant. For matching purposes it is worthwhile to determine θ up to one more order

$$\begin{aligned}\theta_2 \;=\; & \frac{I(s) + s\log(\cos s)}{24} \\ & + \sec^2 s \left\{ \frac{(1+24c_1)s}{96} + \frac{(1+8c_1)s\cos 2s}{32} \right. \\ & \qquad \left. + \frac{s\cos 4s}{96} - \frac{29\sin 2s}{1152} - \frac{7\sin 4s}{576} + \frac{\sin 6s}{1152} \right\},\end{aligned} \tag{B8}$$

where

$$I(s) = \int_0^s \xi\tan\xi\,\mathrm{d}\xi. \tag{B9}$$

This asymptotic solution is clearly nonuniform near $s = \pi/2$ (*i.e.* the top of the bubble). Although it will transpire that the region in which validity breaks down is outside the domain of interest to the current problem, to confirm that our asymptotic solution is self-consistent we perform a local analysis of this point, setting

$$s = \pi/2 + \mathrm{B}\xi, \qquad \theta(s) = \alpha(\xi), \qquad \eta(s) = \mathrm{B}Y(\xi), \qquad r(s) = \mathrm{B}R(\xi). \tag{B10}$$

Hence the problem for α, Y and R reads

$$\frac{\partial\alpha}{\partial\xi} + \frac{\sin\alpha}{r} = 4\mathrm{B} + \mathrm{B}^3 Y, \qquad \frac{\partial Y}{\partial\xi} = \sin\alpha, \qquad \frac{\partial R}{\partial\xi} = \cos\alpha, \tag{B11}$$

and the leading-order solution is

$$\alpha_0 = 3\pi/2 - \tan^{-1}(a_2 - a_1\xi), \tag{B12}$$

$$Y_0 = a_3 + \frac{\sinh^{-1}(a_2 - a_1\xi)}{a_1}, \tag{B13}$$

$$R_0 = \frac{\sqrt{1 + (a_2 - a_1\xi)^2}}{a_1}, \tag{B14}$$

where the constants of integration a_i have to be determined by matching with the outer solution. First we take the three-term outer solution for θ and expand in inner variables up to one term

$$\theta \sim \pi - \frac{1}{12\xi} - \frac{\pi}{192\xi^2}, \tag{B15}$$

using the expansion

$$I(\pi/2-\epsilon) \sim \frac{\pi}{2}\log\frac{1}{2\epsilon} + \epsilon + O(\epsilon^3).$$

By comparing this with the three-term outer expansion of (B12) we obtain

$$a_1 = 12, \qquad a_2 = \frac{3\pi}{4}. \tag{B16}$$

Finally we expand the two-term outer solution for η in inner variables,

$$\eta \sim \left(c_1 + \frac{1}{8} + \frac{\log(-\mathrm{B}\xi)}{12}\right)\mathrm{B}, \tag{B17}$$

and by comparing with (B13), obtain

$$a_3 = c_1 + \frac{1}{8} + \frac{\log(\mathrm{B}/24)}{12}. \tag{B18}$$

We have obtained self-consistent asymptotic approximations to the 'inside' free-surface profile. It remains to fit this free surface to a spherical cap of unit radius. To do so we require

$$r = \sin\theta \quad \text{at (say)} s = s_c. \tag{B19}$$

By comparing the expansions for r and θ, we see that this condition can only be satisfied if $s_c - \pi/2 \sim O(\sqrt{\mathrm{B}})$, so that, as noted earlier, the contact point occurs in a region in which our outer expansion is valid. Substituting the expansions for r and θ into (B19) and posing an expansion for s_c in powers of $\sqrt{\mathrm{B}}$, we find that

$$s_c \sim \frac{\pi}{2} - \frac{\sqrt{\mathrm{B}}}{2\sqrt{3}} + \frac{\pi\mathrm{B}}{16} + O(\mathrm{B}^{3/2}). \tag{B20}$$

Moreover, we obtain the free-surface angle and height at the contact point

$$\theta_c = \theta(s_c) - \pi \sim -\frac{\sqrt{\mathrm{B}}}{2\sqrt{3}} + O(B^{3/2}), \tag{B21}$$

$$\eta_c = \eta(s_c) \sim \left\{1 + 24c_1 + \log\frac{\mathrm{B}}{12}\right\}\frac{B}{24} + O(\mathrm{B}^{3/2}\log\mathrm{B}), \tag{B22}$$

where now only the constant c_1 remains to be determined. We do so in the next section by examining the outside surface.

B2. The 'outside' surface

The general equations to be satisfied by the free surface outside the bubble are

$$\frac{\partial\theta}{\partial s} + \frac{\sin\theta}{r} = \mathrm{B}\eta, \qquad \frac{\partial\eta}{\partial s} = \sin\theta, \qquad \frac{\partial r}{\partial s} = \cos\theta. \tag{B23}$$

We start in a neighbourhood of the contact point and scale as suggested by (B21, B22),

$$\begin{aligned} s &= \sqrt{\mathrm{B}}\varsigma, \qquad \theta(s) = \sqrt{\mathrm{B}}\phi(\varsigma), \\ \eta(s) &= \mathrm{B}\zeta(\varsigma), \qquad r(s) = \sqrt{\mathrm{B}}\rho(\varsigma), \end{aligned} \tag{B24}$$

so the leading-order equations are

$$\frac{\partial\phi_0}{\partial\varsigma} + \frac{\phi_0}{\rho} = 0, \qquad \frac{\partial\zeta_0}{\partial\varsigma} = \phi_0, \qquad \frac{\partial\rho_0}{\partial\varsigma} = 1. \tag{B25}$$

Using (B21, B22) as initial conditions, we obtain

$$\phi_0 = -\frac{1}{12\varsigma}, \qquad \zeta_0 = \frac{1 + 24c_1 + \log\mathrm{B} - 2\log(12\varsigma)}{24}, \qquad \rho_0 = \varsigma. \tag{B26}$$

The logarithmic blow-up of the free surface (not surprising in an axisymmetric geometry) is counteracted by gravity in the far field. To examine this, rescale as follows,

$$\varsigma = \frac{\Sigma}{\mathrm{B}}, \qquad \phi(\varsigma) = \mathrm{B}\Phi(\Sigma), \qquad \zeta(\varsigma) = Z(\Sigma), \qquad \rho(\varsigma) = \frac{R(\Sigma)}{\mathrm{B}}, \tag{B27}$$

so that the leading-order equations become

$$\frac{\partial\Phi_0}{\partial\Sigma} + \frac{\Phi_0}{R_0} = Z_0, \qquad \frac{\partial Z_0}{\partial\Sigma} = \Phi_0, \qquad \frac{\partial R_0}{\partial\Sigma} = 1. \tag{B28}$$

The solution that matches to leading order with (B26) is (as in [27])

$$\Phi_0 = \frac{\mathrm{K}_1(\Sigma)}{12}, \tag{B29}$$

$$Z_0 = \frac{\mathrm{K}_0(\Sigma)}{12}, \tag{B30}$$

$$R_0 = \Sigma, \tag{B31}$$

where the K_i denote modified Bessel functions. An expansion of (B30) in inner variables gives

$$Z \sim \frac{\log 2 - \log(\mathrm{B}\varsigma) - \gamma}{12}, \tag{B32}$$

where γ is Euler's constant. By comparing this with (B26) we finally obtain the constant c_1,

$$c_1 = \frac{2\log 24 - 3\log\mathrm{B} - 1 - 2\gamma}{24}, \tag{B33}$$

and hence the height of the intersection point,

$$\eta_c \sim \frac{\mathrm{B}}{24}\{\log 24 - 2\log\mathrm{B} - 2\gamma\} + O(\mathrm{B}^{3/2}\log\mathrm{B}). \tag{B34}$$

As in Section 2, for matching with the thin film we require the total curvature of the two free surfaces at their point of intersection, and once again this is given by

$$\kappa_{\text{total}} = 2(1 + \mathrm{B}\eta_c). \tag{B35}$$

B.3. The thin film

We use the thin-film equations given in Appendix A in axisymmetric form. As in Section 2, the normal force balance simply tells us that the film has constant mean curvature to leading order and, in an axisymmetric geometry, this implies that it is a spherical cap, as assumed in Section B.1. Therefore we use spherical polar coordinates to describe flow in the cap, with the dimensionless centre-surface given by

$$\boldsymbol{r} = \boldsymbol{r}_c(\theta, \psi) = \begin{pmatrix} \sin\theta\cos\psi \\ \sin\theta\sin\psi \\ \cos\theta \end{pmatrix}. \tag{B36}$$

Assuming that the flow is independent of ψ, and nondimensionalising all lengths with R, we observe that the film thickness h and velocity in the θ-direction u satisfy

$$\frac{\partial h}{\partial t} + \frac{1}{\sin\theta}\frac{\partial}{\partial\theta}(uh\sin\theta) = 0, \tag{B37}$$

$$\begin{aligned}&\mathrm{Ca}\left\{\frac{\partial}{\partial\theta}\left[2h\left(2\sin\theta\frac{\partial u}{\partial\theta} + u\cos\theta\right)\right] - 2h\cos\theta\left(\frac{\partial u}{\partial\theta} + 2u\cos\theta\right)\right\} \\ &\quad + \frac{\epsilon}{2}\sin\theta\frac{\partial}{\partial\theta}\left[\frac{1}{\sin\theta}\frac{\partial}{\partial\theta}\left(\sin\theta\frac{\partial h}{\partial\theta}\right) + 2h\right] = \mathrm{B}h\sin^2\theta.\end{aligned} \tag{B38}$$

On the scale of the transition region, the flow is effectively two-dimensional so the results of Section 3.1 can be applied directly. Thus the velocity scale is given by (26) and hence

$$\mathrm{Ca} = \sqrt{\epsilon} = \sqrt{\frac{h_0}{R}}.$$

Also, the length scale of the transition region is given by (25), while from (B21) the diameter of the film is of order $\sqrt{\mathrm{B}}R$. We require that the former be much shorter than the latter, and hence

$$\epsilon \ll \mathrm{B} \ll 1.$$

Then, rescaling over the film length scale,

$$\theta = \sqrt{\mathrm{B}}\phi,$$

the governing equations (B37, B38) reduce to

$$\frac{\partial h}{\partial t} + \frac{1}{\phi}\frac{\partial}{\partial\phi}(uh\phi) = 0, \tag{B39}$$

$$\frac{\partial}{\partial\phi}\left[2h\left(2\phi\frac{\partial u}{\partial\phi}+u\right)\right]-2h\left(\frac{\partial u}{\partial\phi}+\frac{2u}{\phi}\right)$$
$$-\sqrt{\frac{\mathrm{B}^5}{\epsilon}}\phi^2 h\sim O\left(\mathrm{B},\sqrt{\frac{\epsilon}{\mathrm{B}}}\right). \tag{B40}$$

As in Section 3.2, we assume henceforth that the gravity term in (B40) is negligible. The boundary conditions are

$$u=0 \quad \text{at} \quad \phi=0,$$
$$u=\frac{8}{3}\sqrt{\frac{\kappa_{\text{total}}h}{2}} \quad \text{at} \quad \phi=\phi_c, \tag{B41}$$

where

$$\phi_c\sim\frac{1}{2\sqrt{3}}+O(\mathrm{B}), \qquad \kappa_{\text{total}}\sim 2+O(\mathrm{B}^2\log\mathrm{B}),$$

plus an initial condition for h. Again, the problem is particularly easy to solve if h is uniform initially, since then it remains spatially uniform. In this case its evolution is given dimensionally by

$$\frac{h}{h_0}=\left(1+\frac{16}{\sqrt{3}}\frac{\sigma^{3/2}}{\mu\sqrt{\rho g}}\frac{h_0^{1/2}}{R^{5/2}}t\right)^{-2}, \tag{B42}$$

and the dimensional rupture time as

$$t_{\text{rup}}=\frac{\sqrt{3}}{16}\frac{\mu\sqrt{\rho g}}{\sigma^{3/2}}R^2\left(\sqrt{\frac{R}{h_{\text{rup}}}}-\sqrt{\frac{R}{h_0}}\right). \tag{B43}$$

As in the two-dimensional calculation, using the estimated parameter values given in Table 1, t_{rup} is approximately one minute.

References

1. A. F. Jones and S. D. R. Wilson, The film drainage problem in droplet coalescence. *J. Fluid Mech.* 87 (1978) 263–288.
2. B. K. Chi and L. G. Leal, A theoretical study of the motion of a viscous drop toward a fluid interface at low Reynolds number. *J. Fluid Mech.* 201 (1989) 123–146.
3. P. J. Shopov and P.D. Minev, The unsteady motion of a bubble or drop towards a liquid-liquid interface. *J. Fluid Mech.* 235 (1992) 123–141.
4. R. Wu and S. Weinbaum, On the development of fluid trapping beneath deformable fluid-cell membranes. *J Fluid Mech.* 121 (1982) 315–343.
5. C.-Y. Lin and J. C. Slattery, Thinning of a liquid film as a small drop or bubble approaches a fluid-fluid interface. *AIChE J.* 28 (1982) 787–792.
6. S. G. Yiantsios and R. H. Davis, On the buoyancy-driven motion of a drop towards a rigid surface or a deformable interface. *J. Fluid Mech.* 217 (1990) 547–573.
7. J.-D. Chen, P. S. Hahn and J. C. Slattery, Coalescence time for a small drop or bubble at a fluid-fluid interface. *AIChE J.* 30 (1984) 622–630.

8. P.-S. Hahn, J.-D. Chen and J. C. Slattery, Effects of London-van der Waals forces on the thinning and rupture of a dimpled liquid film as a small drop of bubble approaches a fluid-fluid interface. *AIChE J.* 31 (1985) 2026–2038.
9. T. G. Myers, Thin films with high surface tension. *SIAM Rev.* 40 (1998). To appear.
10. P. D. Howell, Models for thin viscous sheets. *Eur. J. Appl. Maths* 7 (1996) 321–343.
11. J. R. A. Pearson and C. J. S. Petrie, The flow of a tubular film Part 1. Formal mathematical representation. *J. Fluid Mech.* 42 (1970) 609–625.
12. B. W. van de Fliert, P. D. Howell and J. R. Ockendon, Pressure-driven flow of a thin viscous sheet. *J. Fluid Mech.* 292 (1995) 359–376.
13. T. Erneux and S. H. Davis, Nonlinear rupture of free films. *Phys. Fluids A* 5 (1993) 1117–1122.
14. C.-C. Hwang, J.-L. Chen, L.-F. Shen and C.-I. Weng, Strong nonlinear rupture theory of thin free liquid films. *Physica A* 231 (1996) 448–460.
15. M. P. Ida and M. J. Miksis, Dynamics of a lamella in a capillary tube. *SIAM J. Appl. Math.* 55 (1995) 23–57.
16. M. P. Ida and M. J. Miksis, Thin-film rupture. *Appl. Math. Lett.* 9 (1996) 35–40.
17. A. De Witt, D. Gallez and C. I Christov, Nonlinear evolution equations for thin liquid films with insoluble surfactants. *Phys. Fluids* 6 (1994) 3256–3266.
18. C.-C. Hwang, J.-L. Chen and L.-F. Shen, Nonlinear rupture theory of a thin free liquid film with insoluble surfactant. *J. Phys. Soc. Japan* 65 (1996) 2494–2501.
19. F. P. Bretherton, The motion of long bubbles in tubes. *J. Fluid Mech.* 10 (1961) 166–188.
20. H. Lamb, *Hydrodynamics*, sixth edition. Cambridge University Press (1932) 738pp.
21. G. K. Batchelor, *Fluid Dynamics*. Cambridge University Press (1967) 615pp.
22. S. Richardson, Two-dimensional slow viscous flows with time-dependent free boundaries driven by surface tension. *Eur. J. Appl. Maths* 3 (1992) 193–207.
23. C. J. W. Breward, R. C. Darton, P. D. Howell and J. R. Ockendon, Modelling foam drainage. In: R, C, Darton (ed.), *Distillation and Absorption '97*, volume 2. Rugby, UK: Institution of Chemical Engineers (1997) pp.1009–1019.
24. R. Aris, *Vectors, Tensors, and the basic Equations of Fluid Mechanics*. Dover, (1962) 286pp.
25. S. B. G. O'Brien, On the shape of small sessile and pendant drops by singular perturbation techniques. *J. Fluid Mech.* 233 (1991) 519–537.
26. D. F. James, The meniscus on the outside of a small circular cylinder. *J. Fluid Mech.* 63 (1974) 657–664.
27. L. L. Lo, The meniscus on a needle – a lesson in matching. *J. Fluid Mech.* 132 (1983) 65–78.
28. S. K. Wilson and B. R. Duffy, An asymptotic analysis of small holes in thin fluid layers. *J. Engng Maths* 30 (1996) 445–457.